AFCRL-62-364

Final Report

January 1, 1961 - January 1, 1962

INVESTIGATION OF HIGH FREQUENCY

GASEOUS BREAKDOWN UNDER CONDITIONS

OF NON-UNIFORM ELECTRIC FIELDS

Contract No. AF19(604)-7388

Prepared by:

Harvey Fields

Approved by:

Dr. Grant E. St. John

MICROWAVE ASSOCIATES, INC.
Burlington, Massachusetts

TABLE OF CONTENTS

ABSTRACT

A study of microwave breakdown in strongly non-uniform electric fields has been performed. Breakdown fields in air have been measured in three resonant cavities at X-band frequencies. One cavity was designed to provide uniform field breakdown, while the other two had strong field gradients. Effective diffusion lengths for the non-uniform field cavities were calculated, by making use of the variational theory for non-uniform field breakdown. The experimental results for the uniform field cavity are in good agreement with theory; however, the observed data for the non-uniform field cavities shows only fair agreement with theory. The discrepancy between theory and experiment in the diffusion region is not unexpected, considering the assumptions that were made in the theory. However, the discrepancy in the attachment region of the experiments is unexpected and suggest the possibility that an additional mechanism may play a significant role in non-uniform field breakdown.

I. INTRODUCTION

The electrical breakdown of gases at microwave frequencies has
been studied by a number of authors in the past.[1-7] C.W. breakdown
is defined as the condition which exists in the gas at the instant of
time when the rate at which electrons are being lost is exactly balanced
by the rate at which they are created. The loss of electrons is accom-
plished by the mechanisms of diffusion, attachment and recombination.
Their production is due to ionizing collisions by electrons which have
gained sufficient energy from the applied electric field. The pressure,
container size, and the characteristics of the gas determine which loss
process is dominant.

The C.W. breakdown condition is expressed analytically, by the
steady state continuity equation. For diffusion controlled breakdown,
this equation is solved subject to the boundary condition that the elec-
tron density vanishes at the walls of the container. If the electric
field is uniform in space, the governing equation is a second order,
linear, homogeneous differential equation with constant coefficients,
whose solution is straightforward. An infinite number of eigenvalues
is obtained corresponding to an infinity of solutions for the electron
density distribution. Each solution refers to a diffusion mode, but
only those combinations of solutions, which are everywhere psoitive,
are admissible. In breakdown experiments it is the lowest eigenvalue
which enters the calculations. This is based on the assumption that the
lowest diffusion mode dominates breakdown.

In analogy to the first Townsend coefficient for d.c. breakdown,

a high frequency ionization coefficient is defined

$$\zeta = \frac{\nu}{D \ E^2} \qquad (1)$$

Here, ν is the net production rate per electron, D is the diffusion
coefficient and E the electric field. The quantity ζ is thus a
function of electron energy as both ν and D are energy dependent
quantities. The energy dependence of ζ is expressed as a functional
relation between ζ and E/p, where p is the pressure and E/p is the
proper energy parameter. If this functional relation is known then
the breakdown field can be determined by relating the lowest eigenvalue
to the high frequency ionization coefficient. This leads to

$$\zeta = \frac{1}{(\Lambda E)^2} \qquad (2)$$

where Λ is the characteristic diffusion length of the container.

The energy dependence of the ionization coefficient is, in general,
arrived at, by making use of the Boltzman transport equation and kinetic
theory.[2] The Boltzman transport equation yields the electron energy
distribution function. Kinetic theory relates the distribution function
to the ionization frequency and to the diffusion coefficient. However,

the complexity of the calculations limits the applicability of this approach to those few gases which exhibit relatively simple properties. The properties of the gas that determine the complexity of the calculations are the energy dependences of the cross-sections for the various elastic and inelastic processes that may occur. Even for simple gases such as He, or H_2 approximations are necessary.

Another approach in arriving at the energy dependence of the high frequency ionization coefficient, is to make use of available d.c. experimental data. This approach has been successfully applied to air where the data, for the energy dependence of the coefficients for ionization and attachment is available.

Once the high frequency ionization coefficient is known, the problem is essentially solved for the case of uniform fields. Almost all of the workers in the past have so designed their experiment that the breakdown field was uniform in the direction in which diffusion took place.

The effect of a non-uniform field on breakdown has also been studied by a number of authors.[8-11] An effective diffusion length is arrived at by solving the diffusion equation for the case of a non-uniform field. Herlin and Brown[3] have solved this equation approximately for a few simple cases in terms of confluent hypergeometric functions. Buchsbaum[9] has shown that a variational technique can be applied to this problem, and both he and the author[10] have used this technique in some simple cases. More recently, Platzman and Solt[11] have used the variational method in a more general case and have

achieved good agreement with experimental results. In this work, we
applied the variational method to conditions having an essential
difference from those of Platzman and Solt.[11] While they studied
primarily the effect of non-uniform fields on electrical breakdown at
small metallic discontinuities, we studied the effect of the non-uniform
fields found in higher order mode cavities. Thus within the volume,
remote from the walls, there existed regions of where the electric field
was too small to cause net ionization.

II. THEORY FOR BREAKDOWN IN NON-UNIFORM ELECTRIC FIELDS[11]

A. Solution of the Diffusion Equation

The differential equation that governs C.W. diffusion controlled breakdown is[1]

$$\nabla^2 \psi + \zeta E^2 \psi = 0,$$ (3)

where $\psi = Dn$, n being the electron number density. If E is uniform, ζ and D are independent of position and the equation is easily solved subject to the boundary condition that n vanishes at the walls of the container. This leads to the lowest eigenvalue given by

$$k^2 = \zeta E^2$$ (4)

The eigenvalue k is the reciprocal of the diffusion length Λ, which is determined by the geometry of the container. If ζ is known as a function of E then the breakdown field is given by (4).

If the field is not uniform in space, then it can be expressed as

$$E = E' \, F(x,y,z)$$ (5)

where E' is the value of the field at a particular point in the region. The value of ζ at this point is designated as ζ'. The characteristic value is then expressed as

$$k^2 = \zeta E^2 = \zeta' E'^2 \left(\frac{\zeta}{\zeta'}\right) \left(\frac{E}{E'}\right)^2 \tag{6}$$

where $$k'^2 = \zeta' E'^2 \tag{7}$$

Assuming that the diffusion coefficient D is a slowly varying function with energy, (so that its space dependence can be neglected, except insofar as it is taken account of in the space variation of ζ) then Equation (3) is still valid for non-uniform field breakdown, and substitution of (6) into (3) yields

$$\nabla^2 n + k'^2 \left(\frac{\zeta}{\zeta'}\right) \left(\frac{E}{E'}\right)^2 n = 0 \tag{8}$$

The problem is to determine the new eigenvalue k' which together with Equation (7) determines the breakdown field E'.

Equation (8) is still linear and homogeneous, however, the

coefficients are no longer constant, but depend on the independent space variables. The equation is solved by using the variational method. We rewrite (8) as

$$k'^2 = -\int n\nabla^2 n dv \Big| \int n^2 \left(\frac{\zeta}{\zeta'}\right) \left(\frac{E}{E'}\right)^2 dv \qquad (9)$$

where the integration is carried out over the total volume of the container. By making use of the identity

$$\nabla \cdot (r\nabla n) = \nabla n . \nabla n + n\nabla^2 n \qquad (10)$$

and of Green's theorem, together with the condition that n vanishes at the boundary of the container, Equation (9) reduces to

$$k'^2 = \int (\nabla n)^2 dv \Big| \int n^2 \left(\zeta/\zeta'\right) \left(\frac{E}{E'}\right)^2 dv \qquad (11)$$

The next step is to use a theorem which is proven in the theory of the calculus of variations. The theorem states that if an n satisfies Equation (8) and either one of two boundary conditions, i.e., either

n or its normal derivative vanishes at the walls, then it must also satisfy the equation

$$\zeta(k'^2) = 0, \tag{12}$$

where ζ indicates minimization of Equation (11) with respect to variation in n. In addition, k'^2 will have an absolute minimum corresponding to the lowest eigenvalue if (ζ/ζ') is nowhere negative.

The method then involves choosing a trial function for n which contains one or more arbitrary parameters. The form of the trial function is usually suggested by the physical situation. The quantity k'^2 is minimized with respect to the variational parameters, and its minimum value will be an upper bound on the lowest eigenvalue. This method leads to an approximate lowest eigenvalue, the accuracy of the approximation being determined by the accuracy with which the trial solution approximates the actual electron density distribution.

Equation (7) can be rewritten as

$$\left(\frac{k'}{p}\right)^2 = \left(\frac{1}{p\Lambda'}\right)^2 = \zeta'\left(\frac{E'}{p}\right)^2 \tag{3}$$

where Λ' is an effective diffusion length for non-uniform field

breakdown. Unlike the uniform field case where the diffusion length is determined solely by the geometry, Λ' is now a function of E/p. This is seen from Equation (11) where the quantity (ζ/ζ') is functionally related to E/p. It is through this relation that the space dependence of (ζ/ζ') is determined and used in (11). Once Λ' has been determined as a function of E/p for a particular field non-uniformity, Equation (13) together with the relation between ζ and E/p, leads to a plot of E'/p vs. $p\Lambda'$. The experimental results can then be compared to this theoretical curve by using the calculated Λ' corresponding to each experimental value of E'/p.

B. **Determination of the High Frequency Ionization Coefficient**

Several factors, to be discussed subsequently, dictated the choice of air as the gas fill to be studied. The high frequency ionization coefficient for air is determined from d.c. data by writing[6,7]

$$\zeta = \frac{3}{2} \frac{\alpha/p - \beta/p}{u_{av}} \tag{14}$$

In this expression α = number of ionizing collisions per cm per electron, β = number of attaching collisions per cm per electron and u_{av} is the average electron energy. Recombination losses at breakdown densities in air can be neglected, and are therefore not included in (14). The experimental data for the dependence of α/p, β/p and u_{av} on E_{dc}/p is

used to calculate ζ as a function of E_{dc} p. The result can be applied
to high frequency fields if instead of the d.c. field an equivalent
high frequency field is used. The equivalent field E_{eq} is defined as[6],[12]

$$E_{eq}/p = E_e/p + \Delta \tag{15}$$

where

$$E_e{}^2 = E_{rms}^2 / \left[1 + (\omega/\nu_c)^2 \right], \tag{16}$$

E_e is an effective field, E_{rms} = r.m.s. value of the high frequency
field, ω = radian frequency of the high frequency field, ν_c = electron-
molecule collision frequency and Δ is a term that takes account of the
electron energy modulation. This term is important only at high pres-
sures when the energy relaxation time becomes comparable to the r.f.
period. In comparing theory with experiment the experimental break-
down fields must be reduced to this equivalent field, which results in
the same net ionization as a d.c. field of the same magnitude.

The high frequency ionization coefficient for air has been calcu-
lated by Platzman and Solt.[11] We used these results in calculating the
effective diffusion lengths for our experimental conditions. In reduc-
ing the experimental data, the results of Gould and Roberts[6] were used
for the energy modulation term Δ.

C. Limits of Applicability of the Theory

In Section II A we have seen that the calculation of effective diffusion lengths involves a knowledge of the dependence of ζ on E/p. In calculating ζ from kinetic theory one usually gets a dependence on three parameters, E/p, $p\lambda$ and Λ/λ where λ is the wavelength of the high frequency field. The dependence on Λ is due to the assumption[1] that $\nabla^2 f_o = -f_o/\Lambda^2$, where f_o is the electron energy distribution function. The assumption is made in order to facilitate the solution of the Boltzman equation for f_o. Since it is the diffusion length, applicable to a particular non-uniform field, that we are trying to determine, the method will, in general, be invalid if ζ is a function of Λ. For air this problem does not arise, as ζ is determined from d.c. experimental data and is therefore independent of both λ and Λ.

The theory also is invalid unless the ionization coefficient, and therefore the electron energy at a given point, is determined by the field at that point. This is best seen from Equation (11) where it is necessary to introduce the space dependence of ζ before the variational technique is performed. Since the space dependence of ζ is determined through its dependence on E, the implication is that at a given point ζ is determined by the field at that point. This condition will be satisfied if we experimentally fulfill the two following requirements: (a) The distance that an electron diffuses in an energy relaxation time, and (b) The oscillation amplitude of the electron, are both small compared to the distance over which the field changes appreciably.

The number of collisions that an electron has to make in diffusing

length Λ is[13]

$$\frac{3}{2} \frac{\Lambda^2}{\ell^2} \tag{17}$$

where ℓ is the mean free path of the electron. Therefore the diffusion distance covered in time t will be

$$\Lambda = \left[\frac{2}{3} \ell^2 \nu_c t\right]^{\frac{1}{2}} \tag{18}$$

The mean free path $\ell = \frac{\bar{v}}{\nu_c}$, where $\bar{v}$ is the average electron velocity. Substitution of ℓ leads to

$$\Lambda = \bar{v} \left[\frac{2}{3} \frac{t}{\nu_c}\right]^{\frac{1}{2}} \tag{19}$$

The energy relaxation time can be written as

$$t_r = \frac{1}{(K/p)p^2} \tag{20}$$

where K is the fractional energy lost per second per mm Hg of pressure. The diffusion distance covered by an average electron in a relaxation time is

$$\Lambda = \bar{v} \left[\frac{2}{3} \frac{1}{(K/p)p^2 \nu_c} \right]^{\frac{1}{2}} \tag{21}$$

This must be small compared to an effective diffusion length Λ_e, corresponding to a distance over which the field changes appreciably

$$\bar{v} \left[\frac{2}{3} \frac{1}{(K/p)p^2 \nu_c} \right]^{\frac{1}{2}} < \Lambda_e \tag{22}$$

Assuming a collision frequency of 6×10^9 p and an average electron energy of 5 e.v, leads to the condition that

$$p > \left[\frac{1.5 \times 10^3}{\Lambda_e} \right]^{2/3} \left[K/p \right]^{-1/3} \tag{23}$$

K/p as a function of average electron energy has been computed for air by Gould and Roberts.[*] Using a value of K/p corresponding to 5 e.v,

and an effective diffusion length of 2 x 10^{-3} cm yields,

$$p > 12 \text{ mm of Hg} \tag{24}$$

The value of Λ_e used is one which corresponds to a distance over which the field changes less than 10% over 95% of the cavity volume. The field change will be greater than this, over a similar distance, only in regions of low ionization. This discrepancy should, therefore, not effect the above condition.

The restriction on the pressure given by (24) is stronger than the mean free path condition required for diffusion controlled break-down. For our experimental conditions, the requirement that the mean free path be small compared to the dimension in which diffusion takes place, leads to the condition that $p > 5 \times 10^{-3}$ mm Hg.

The oscillation amplitude limit of the electron is bound from

$$A = \sqrt{2} \, \frac{e}{m} \, \frac{E}{\omega \nu_c} , \tag{25}$$

where A is the oscillation amplitude and $\frac{e}{m}$ is the electron charge to mass ratio. We require that A be small compared to the distance over which the field changes appreciably. For our experimental conditions

we have,

$$\sqrt{2} \; \frac{e}{m} \; \frac{E}{\omega \nu_c} < 5 \times 10^{-5} \tag{26}$$

this leads to the requirement that

$$E/p < 240 \text{ V/cm} - \text{mm Hg} . \tag{27}$$

This condition was satisfied in our experiments.

In addition to these restrictions on the theory, we must consider that the effect we are looking for will be present only in the diffusion controlled pressure region. The theory predicts that the effect of a non-uniform field on breakdown, in a given geometry, is to reduce the diffusion length, thereby raising the required field for breakdown. Since attachment controlled breakdown is independent of geometry, we should not expect to see the non-uniform field effect in this region. From the available data for air[*], it can be seen, that attachment assumes a dominant role at a value of approximately

$$p\Lambda = 6 \text{ cm-mm Hg}. \tag{28}$$

III. EXPERIMENTAL APPARATUS

The heart of the experimental equipment is the microwave cavity in which breakdown fields are measured, as a function of pressure. Three cavities have been used in these experiments. They were made of oxygen free high conductivity copper and were vacuum tight. In appropriate places they had pyrex bubbles which protruded into the cavity, for the purpose of probe coupling microwave power to the cavity. These bubbles were found to limit the pressure range in which data could be taken. At high and low pressures where high powers were needed for breakdown, the bubble overheated thus ruining the coupling to the cavity.

In the design of the cavities the following considerations were the determining factors.

(a) Field configuration

(b) Physical size

(c) Mode separation

The desired field configuration is one which has a strong field gradient in the direction in which most electrons are lost to the walls by diffusion. This requires that the dimension in which a strong field gradient exists, for a particular mode, be small compared to the dimension in which we wish to neglect diffusion. To satisfy this condition for the interesting modes, at S band, would make the physical size of the cavities impractical. The cavities were thus designed to resonate at a frequency of 9.5 Kmc. It is also necessary to insure that other modes

whose resonant frequency is close to 9.5 Kmc will not be excited. The
cavity dimensions separated all undesired modes by at least 50 Mc. In
the one case where this is not so, the coupling probe was placed at a
position in the cavity, where it excited only the desired mode.

All three cavities were right circular cylinders. Their inside
dimensions are given in Figure 1, where we have included a sketch of
a right circular cylinder and a cylindrical co-ordinate system. The
following table gives the mode of oscillation for each cavity together
with the corresponding electric field distribution[14]:

$$
\begin{array}{lll}
1. & TM_{010} & E_Z = J_0 \ (2.405 \ r/R) \\
\\
2. & TM_{020} & E_Z = J_0 \ (5.52 \ r/R) \qquad (30) \\
\\
3. & TE_{011} & E_0 = J_1 \ (3.832 \ r/R) \ \text{Sin} \ \frac{\pi}{L} \ Z
\end{array}
$$

Figure 2 gives a sketch of the electric field distribution in the
direction of major diffusion, for the three cavities.

In Figure 2 it is seen that one cavity has a uniform field in the
direction of major diffusion, while the other two were designed to
have non-uniform fields in the direction of major diffusion. The
data received from the uniform field cavity was used to check our re-
sults with those of previous workers, thus providing a check on the
calibration of the equipment.

The experimental conditions, used in this work to study non-
uniform field breakdown, differ from those of Platzman and Solt[11] in
two respects:

a) There is a strong field gradient in the direction of major diffusion, which should result in an increased effect. This was accomplished without change in the geometry. Platzman and Solt[11] created strong gradients in a small region of the cavity, by introducing a small boss in the center of their cavity. This would have the effect of changing the diffusion length even if the field were to remain uniform. It is possible that the discrepancy between theory and their data, for the pressure range where the boss was effective, is due to this additional effect.

b) The cavity oscillating in the TE_{011} mode has a field distribution that is periodic in the direction of major diffusion. If the data and calculations for this cavity should show a relation between the effective diffusion length and the spacial periodicity, then it may be possible to relate effective diffusion lengths for breakdown in unbounded regions to the wavelength of the breakdown field. Such a relation would be a function of the parameter E/p, due to the dependence of the effective diffusion length on E/p.

The arrangement of the apparatus in the experiment is shown in the block diagram of Figure 3. The equipment is standard and is similar to that used in previous breakdown experiments.[1-7] We used a one millicurie radiation source to provide initial electrons for the start of the breakdown avalanche.

The experimental procedure consisted of measuring the power absorbed by the cavity at breakdown for various pressures. From this data together with a measurement of the Q of the cavity, the maximum field in

the cavity at breakdown was determined.[15],[16] Breakdown was noted by observing a sudden increase in the VSWR of the cavity at resonance.

IV. MEASUREMENTS OF Q

Figures 4 through 10 present the data of measurements of voltage standing wave ratios and positions of voltage minima as a function of frequency for the three cavities. This data, together with the theoretical charts of Brown and Rose,[16] was used to determine the Q of the cavities.

The loaded Q is defined as

$$Q_L = \frac{f_o}{\Delta f} , \tag{31}$$

where f_o is the frequency of resonance and Δf is the width of the VSWR vs. frequency curve. The height at which the width is measured, designated as R_h on the graphs, is determined by the value of the VSWR at resonance (R_o) and the value of the VSWR far away from resonance (R_∞). The unloaded Q can then be determined from the values of Q_L, R_o, R_∞ and from the plot of the position of the voltage minima as a function of frequency. This plot indicates whether the cavity is undercoupled or overcoupled. Figures 6 and 8 show that the cavities resonating in the TM_{010} and TM_{020} modes are undercoupled, while Figure 10 shows the overcoupling of the cavity resonating in the TE_{011} mode. A detailed description of this method of determining the unloaded Q is given in Reference 1.

The following table summarizes the results of the measurments

Mode	f_o (mc)	Δf (mc)	R_o (db)	R_∞ (db)	R_h (db)	Q_L	Q_U
TM_{010}	8851.2	37.3	0.5	29	13.8	237.3	427.1
TM_{020}	9448.2	9.1	2.15	27	13.5	1038.3	1661.2
TE_{011}	9480.5	13.1	7.2	29	15.6	723.7	2272.4

V. DETERMINATION OF THE ELECTRIC FIELD IN THE CAVITY[16]

The power absorbed by the cavity at resonance is related to the energy stored in the cavity by

$$P_o = \frac{\omega_o}{Q_U} u \qquad (32)$$

where ω_o is the radian resonant frequency, Q_U is the unloaded Q and u is the energy stored in the cavity. The stored energy can be expressed as

$$u = \frac{1}{2} \epsilon_o \int_V E^2 \, dv \qquad (33)$$

where ϵ_o is the free space permittivity, E is the electric field in the cavity and the integration is performed over the total volume of the cavity. The electric field can be expressed as

$$E = \sqrt{2} \, E_o \, f \, (r, \theta, z) \qquad (34)$$

where E_O is the rms value of the field at a point in the cavity where the field is a maximum. The function f (r, θ, z) gives the space dependence of the field, as determined by the mode of oscillation. Combining Equations (32), (33), and (34) yields for the power absorbed at resonance

$$P_O = \frac{\omega_O}{Q_U} E_O{}^2 \epsilon_O \int_V f^2 (r, \theta, z) \, dv = \frac{\omega_O}{Q_U} E_O{}^2 \eta \qquad (35)$$

with $\eta = \epsilon_O \int_V f^2 (r, \theta, z) \, dv$.

The rms electric field at the maximum field point can now be written as

$$E_O = \left[\frac{P_O Q_U}{\omega_O \eta} \right]^{\frac{1}{2}} \qquad (36)$$

The following table gives the quantity η for each of the modes considered.

Mode	η
TM_{010}	$0.2695\ \epsilon_0 \pi\ r_0^2 h$
TM_{020}	$0.1158\ \epsilon_0 \pi\ r_0^2 h$
TE_{011}	$0.2395\ \epsilon_0 \pi\ r_0^2 h$

r_0 and h is the radius and height respectively of the cylindrical cavity in each particular case.

If the incident power on the cavity P_1 is measured at resonance, then the absorbed power P_0 is determined from the relation

$$P_0 = P_1\ (1-\rho^2) \tag{37}$$

where ρ is the magnitude of the reflection coefficient at resonance. The desired value of the electric field can then be determined by the use of Equation (36).

VI. DISCUSSION OF RESULTS

Figures 11 through 14 present the results of the calculations for the two non-uniform field cavities. To perform the calculations one assumed an electron density distribution of the form

$$n\ (r,z) = N_o \ \text{Sin} \ \frac{\pi}{L} \ z \ \left[\ |J_o(5.52\ r/R)|\ \right]^m \qquad (38)$$

for the TM_{020} mode cavity, and

$$n\ (r,z) = N_o \ \text{Sin}^m \ \frac{\pi}{L} \ z \ \left[\frac{J_1(3.832\ r/R)}{.5819}\right]^m \qquad (39)$$

for the TE_{011} mode cavity. Here, N_o' is a finite density at the point of maximum field in the cavity and, m is a variational parameter. These expressions together with the $E_{eg}\big/p$ dependence of the ionization coefficient ζ and the electric field distributions in the respective cavities were used in Equation (11) to perform the variational calculations. The calculations were performed on a high speed digital computer. Figures 11 and 12 show the variation of $(k^1/k_o)^2$ with the parameter m and $E_{eg}\big/p$ for the two cavities. Figures 13 and 14 show the variation of the minima of $(k^1/k_o)^2$ with $E_{eg}\big/p$. The minimum k^1 is the

eigenvalue for non-uniform field breakdown or the reciprocal of an effective diffusion length. k_o is the eigenvalue for uniform field breakdown which for a cylindrical cavity is

$$k_o{}^2 = \left(\frac{1}{\Lambda_o}\right)^2 = \left(\frac{\pi}{L}\right)^2 + \left(\frac{2.405}{R}\right)^2 \tag{40}$$

In Figures 11 and 12 we see that the minima of the curves shifts to larger values of m with decreasing E_{eg}/p, indicating a more highly peaked density at lower values of E_{eg}/p. Figures 13 and 14 show the strong E_{eg}/p dependence of the diffusion length for non-uniform field breakdown.

In Figure 15 we compare the data taken in the uniform field TM_{010} cavity with theory. Agreement is good throughout the region where the theory applies, that is down to a value of pressure times gap distance equal to the mean free path limit. The broken line marked $\iota = \Lambda/10$ indicates the mean free path limit for our cavity. The mean free path ι was computed by assuming a mean electron energy of 5 e.v. at breakdown. This is about 1/3 the ionization potential of nitrogen. The broken line marked diffusion limit indicates, roughly, the separation between diffusion and attachment controlled breakdown. In Figure 16 we compare our data for uniform field breakdown with data taken at S band by L. Gould.

The data taken in the two non-uniform field cavities together
with a plot of the theory for uniform field breakdown is shown in
Figure 17. All experimental data was reduced according to Equation (15)
and the diffusion length used in this plot is the one that would apply
if we had uniform field breakdown in the two cavities. Figure 18 pre-
sents the same data after the diffusion length in each case was cor-
rected by the theoretically computed factors given in Figures 13 and
14. In Figure 17 we see that in the diffusion controlled region the
non-uniform breakdown field values do fall above the uniform field
line as expected; that is, any non-uniformity in the field must be
compensated for by an increased value of the maximum field at break-
down. However, in the attachment controlled breakdown, where the loss
mechanism operates in the immediate region where the electron is pro-
duced, one would expect no difference between the non-uniform and
uniform breakdown field values. We would expect the non-uniform field
data to asymptotically approach the attachment limit. Instead the
data indicates that the non-uniform breakdown field values are con-
siderably below the uniform field values in the attachment region.
Furthermore after the corrections to the diffusion lengths have been
applied we would expect that the non-uniform field data to coincide
with the uniform field breakdown data. In Figure 18 we see that the
data falls below the uniform field data.

The discrepancy seen in Figure 18 between theory and experiment
in the diffusion region is not surprising. Our choice for the electron
density spatial distribution in each of the cavities is only a crude

approximation to the actual density distribution. In addition the theory assumes that the ionization coefficient, ζ is determined by the field at each point. This means that the distance that an electron diffuses in an energy relaxation time be small compared to the distance over which the field changes appreciably. We have calculated the pressure below which this is no longer true for our cavities in Section II C. The broken line marked energy relaxation limit in Figure 18 shows this point. At values of $p\Lambda^1$ below this limit the above criteria is not strictly true in our cavities, thus providing an additional cause for the discrepancy of theory and experiment in this region. However, we suspect that the main cause for the discrepancy in this region is the crude choice of the electron density distribution function. A more complex distribution function was not chosen in deference to available computer time.

The fact that the experimental data falls below the attachment limit, suggests that possibly a mechanism in addition to attachment and diffusion plays a role in strongly non-uniform field breakdown. In addition to possible surface effects it is conceivable that a negative space charge near the maximum field point could reduce both diffusion and attachment, thereby lowering the breakdown fields. Such an effect might not have shown up in the uniform field breakdown experiments due to the much larger diffusion rate in the very small gap distance. Should such a space charge exist, it would probably show up stronger in an attaching gas, such as air where negative ions might contribute to the space charge. It is to be noted that the data of Platzman and

Solt[11] for the case of the non-uniformity around a boss, also falls below the theory in the diffusion controlled region. Unfortunately their data does not extend to the attachment controlled region. The possible existence of space charge effects in strongly non-uniform field breakdown warrants further study. It is possible that strong field gradients which can give rise to confining forces, would play a role in the formation of the space charge.
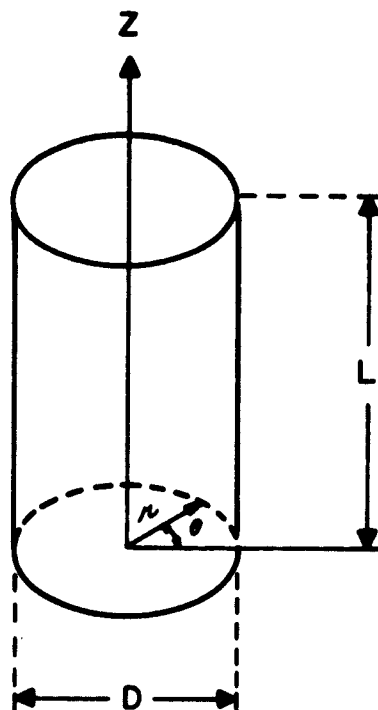
In Section III we mentioned that since the TE_{011} mode cavity has a spacial periodicity in its field distribution, we would look for some relation between this spacial periodicity and effective diffusion length, in the hope of clarifying the choice of one half the wavelength for diffusion lengths in free space. From our calculations no simple relation between the spacial periodicity in the TE_{011} mode cavity and effective diffusion length could be discovered.

REFERENCES

1. M. A. Herlin and S. C. Brown, Phys. Rev. 74, 291 (1948).

2. A. D. MacDonald and S. C. Brown, Phys. Rev. 75, 411 (1949).

3. W. P. Allis and S. C. Brown, Phys. Rev. 87, 419 (1952).

4. A. D. MacDonald and D. D. Betts, Can. J. Phys. 30, 565 (1952); 32, 812 (1954).

5. F. H. Reder and S. C. Brown, Phys. Rev. 95, 885 (1954).

6. L. Gould and L. W. Roberts, J. Appl. Phys. 27, 1162 (1956).

7. D. J. Rose and S. C. Brown, J. Appl. Phys. 28, 561 (1957).

8. M. A. Herlin and S. C. Brown, Phys. Rev. 74, 910 (1948); 74, 1650 (1948).

9. S. J. Buchsbaum, Ph. D. Thesis, Physics Dept. M.I.T. (1957).

10. H. Fields, M. S. Thesis, Physics Dept. M.I.T. (1958).

11. P. M. Platzman and E. H. Solt, Phys. Rev. 119, 1143 (1960).

12. W. P. Allis, Handbuch der Physik, 21, 383 (1956).

13. E. H. Kennard, Kinetic Theory of Gases, McGraw Hill, N. Y. (1938).

14. Montgomery, Technique of Microwave Measurements, McGraw Hill, N. Y. (1938).

15. D. J. Rose and S. C. Brown, J. Appl. Phys. 23, 719 (1952).

16. S. C. Brown and D. J. Rose, J. Appl. Phys. 23, 711 (1952).

LIST OF ILLUSTRATIONS

1.	D = 2.415 cm	L = 0.141 cm
2.	D = 5.545 cm	L = 14.97 cm
3.	D = 3.876 cm	L = 13.407 cm

FIGURE 1
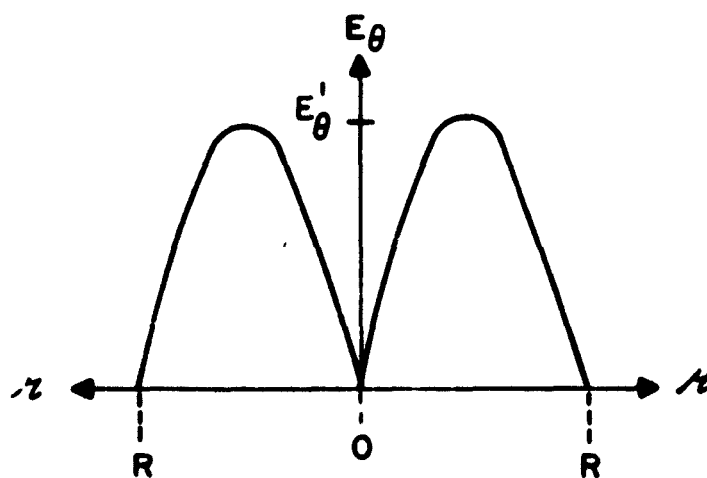## CAVITY DIMENSIONS AND THE RIGHT CIRCULAR CYLINDER.
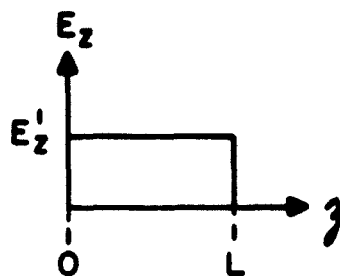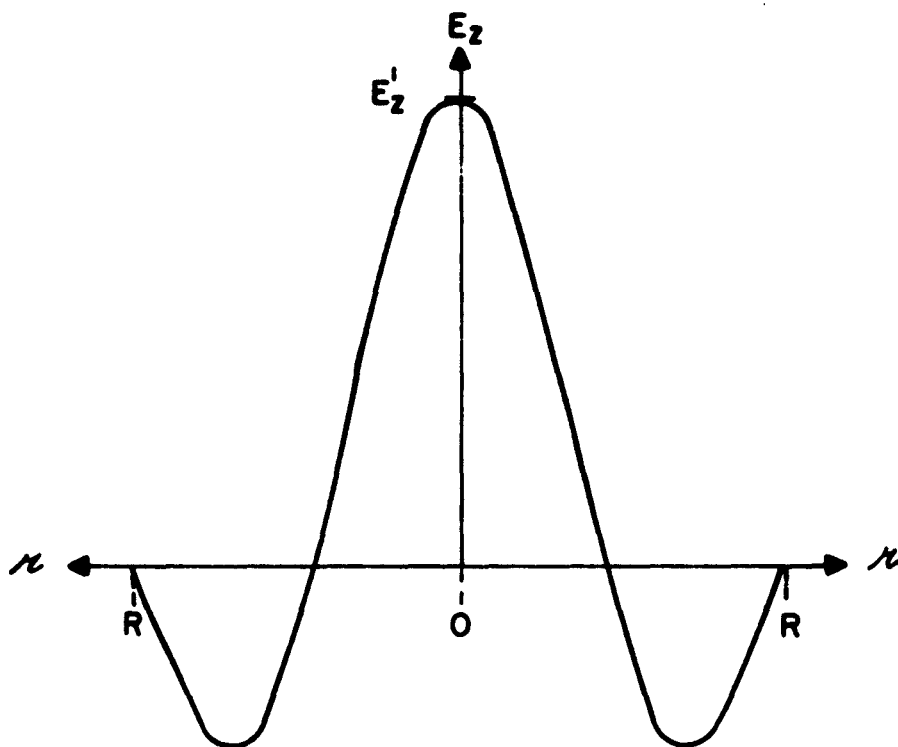
FIGURE 2

ELECTRIC FIELD DISTRBUTION IN THE DIRECTION
OF MAJOR DIFFUSION FOR THE THREE CAVITIES.
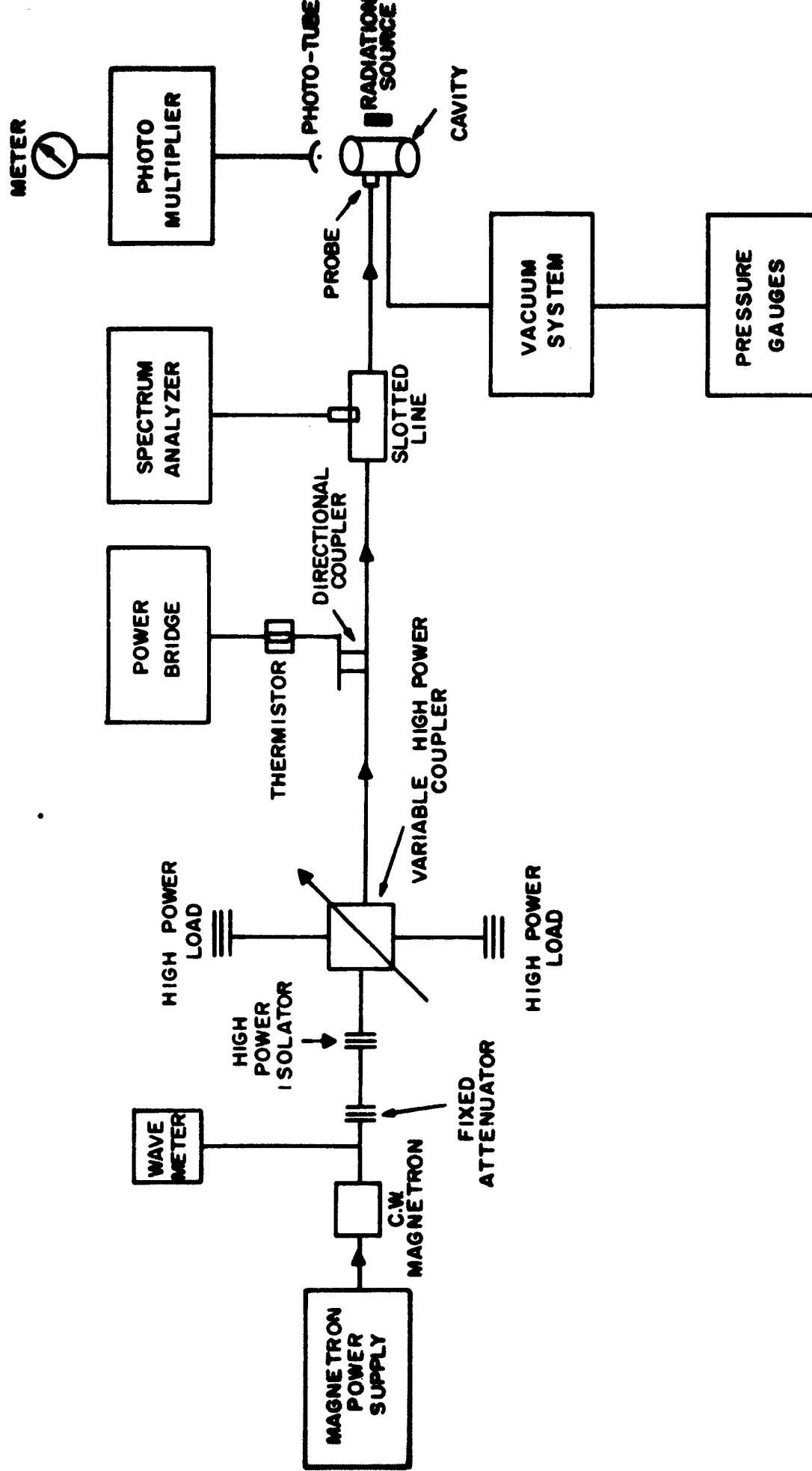
FIGURE 3

BLOCK DIAGRAM OF EXPERIMENTAL APPARATUS

FIGURE 4

VOLTAGE STANDING WAVE RATIO VS.
FREQUENCY, FOR THE CAVITY OSCILLATING
IN THE TM_{010} MODE.

FIGURE 5
VOLTAGE STANDING WAVE RATIO VS. FREQUENCY (EXPANDED SCALE),
FOR THE CAVITY OSCILLATING IN THE TM_{010} MODE.

FIGURE 6
POSITION OF MINIMUM VOLTAGE VS. FREQUENCY, FOR
THE CAVITY OSCILLATING IN THE TM$_{020}$ MODE
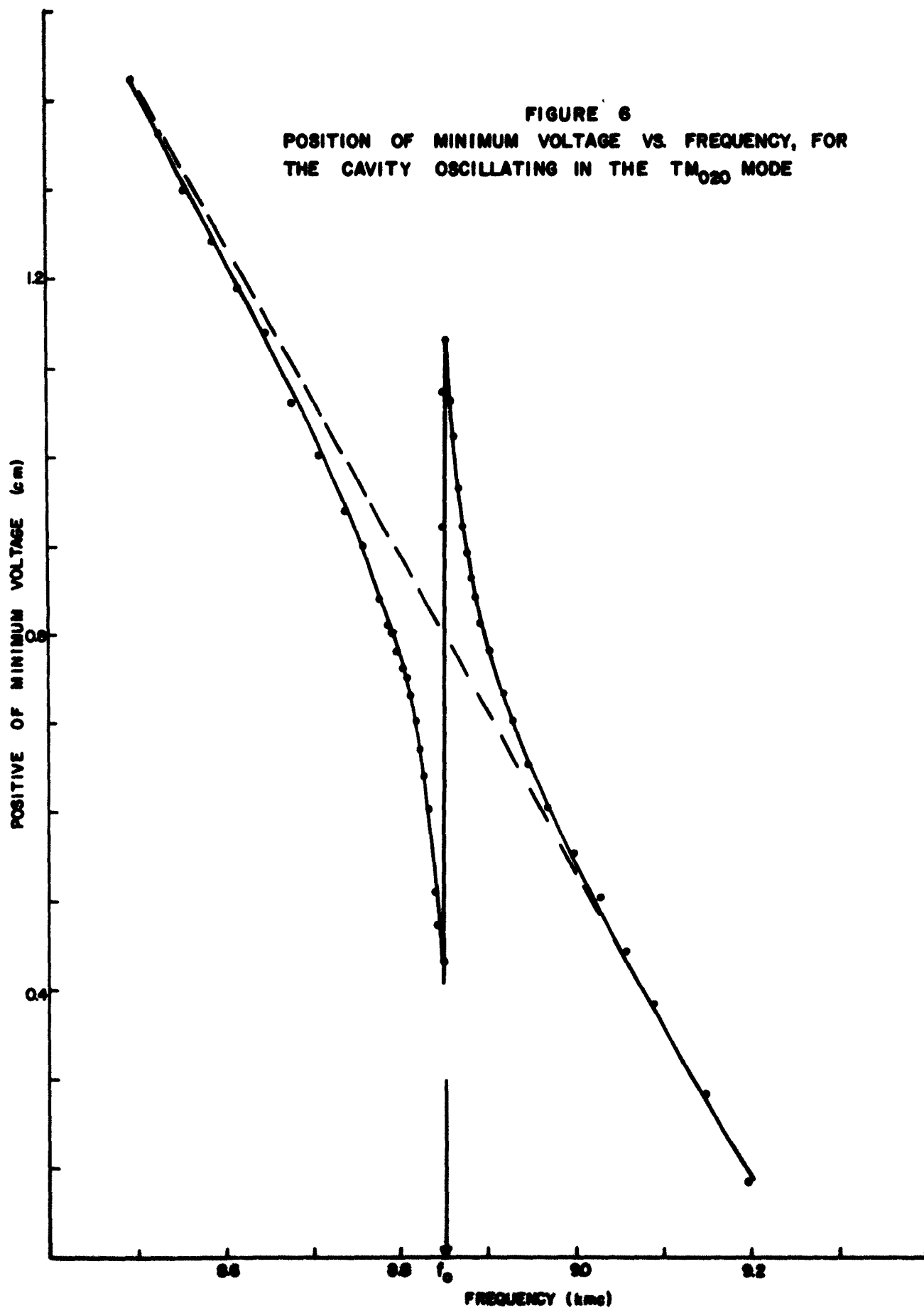
FIGURE 7
VOLTAGE STANDING WAVE RATIO VS. FREQUENCY, FOR
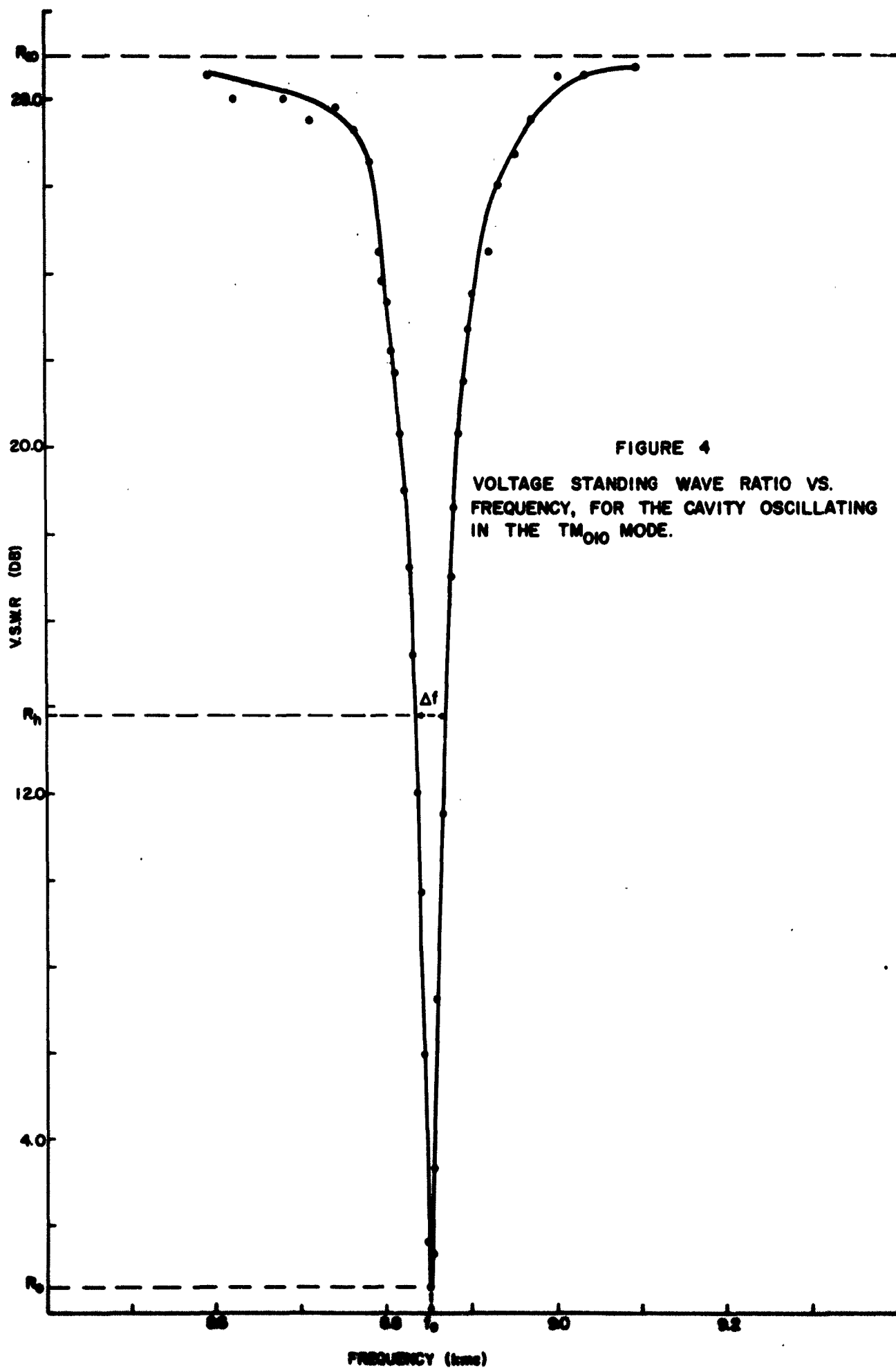THE CAVITY OSCILLATING IN THE TM_{020} MODE
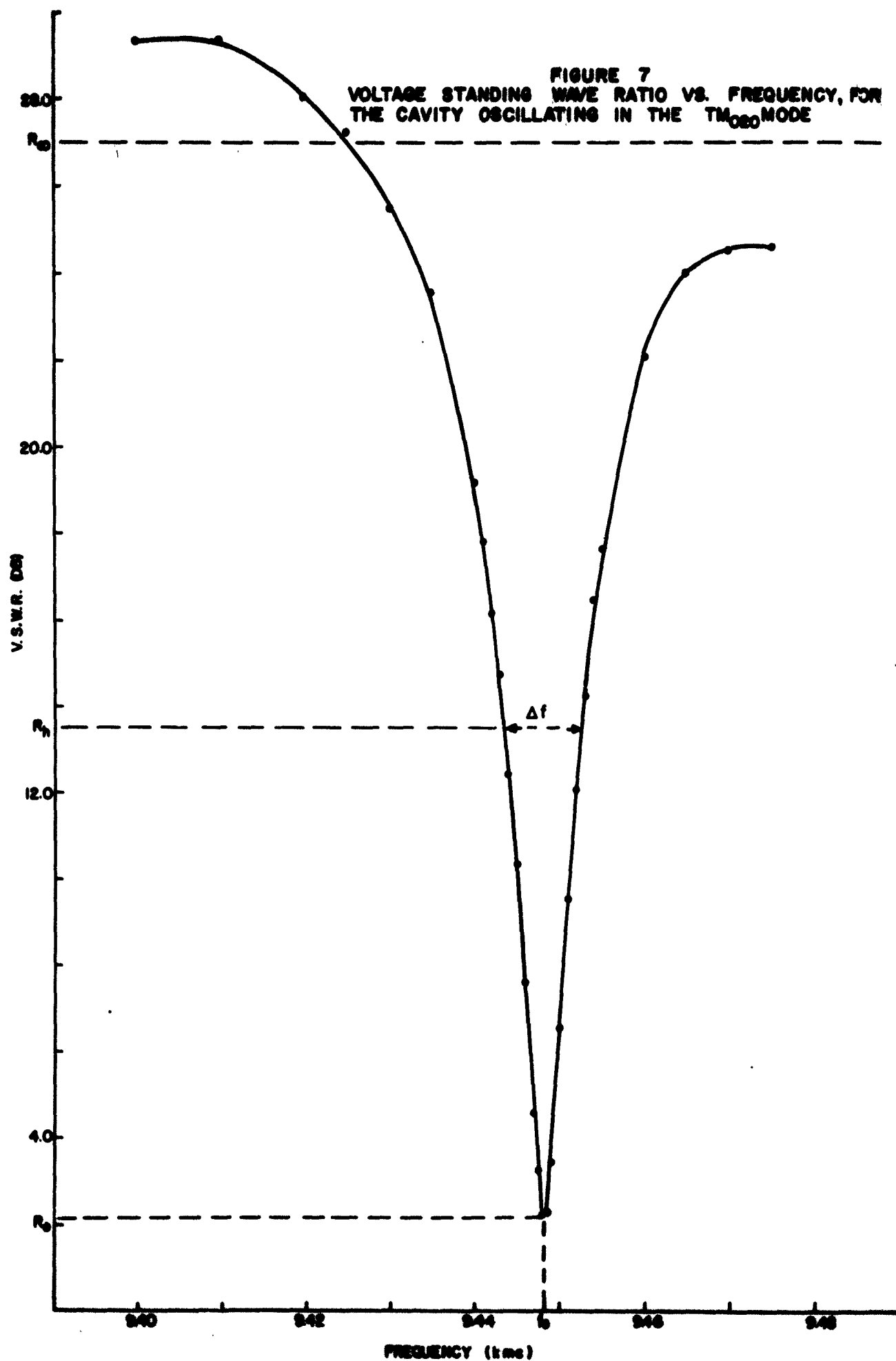
FIGURE 8

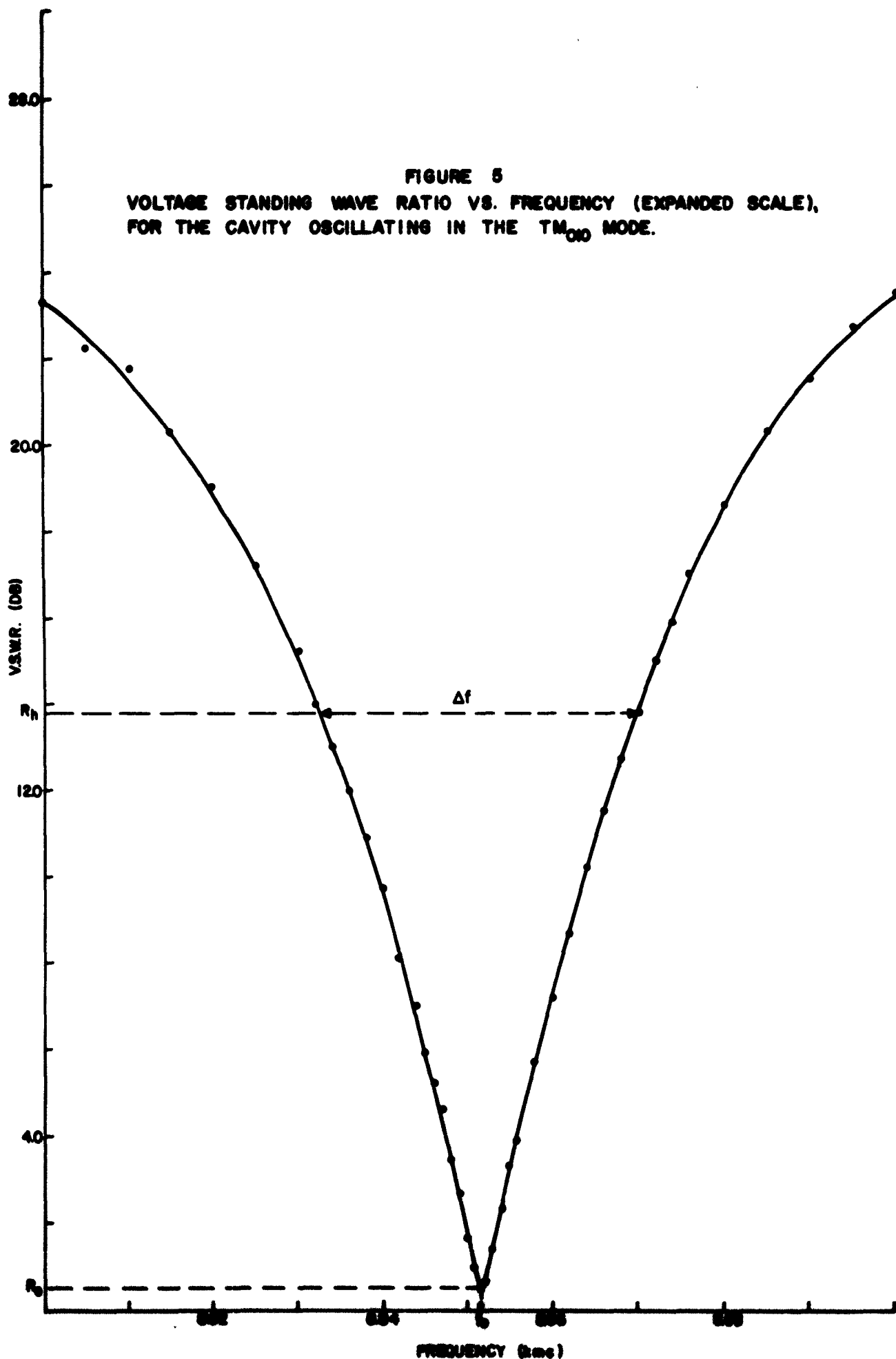POSITION OF MINIMUM VOLTAGE VS. FREQUENCY, FOR THE CAVITY OSCILLATING IN THE TM_{020} MODE
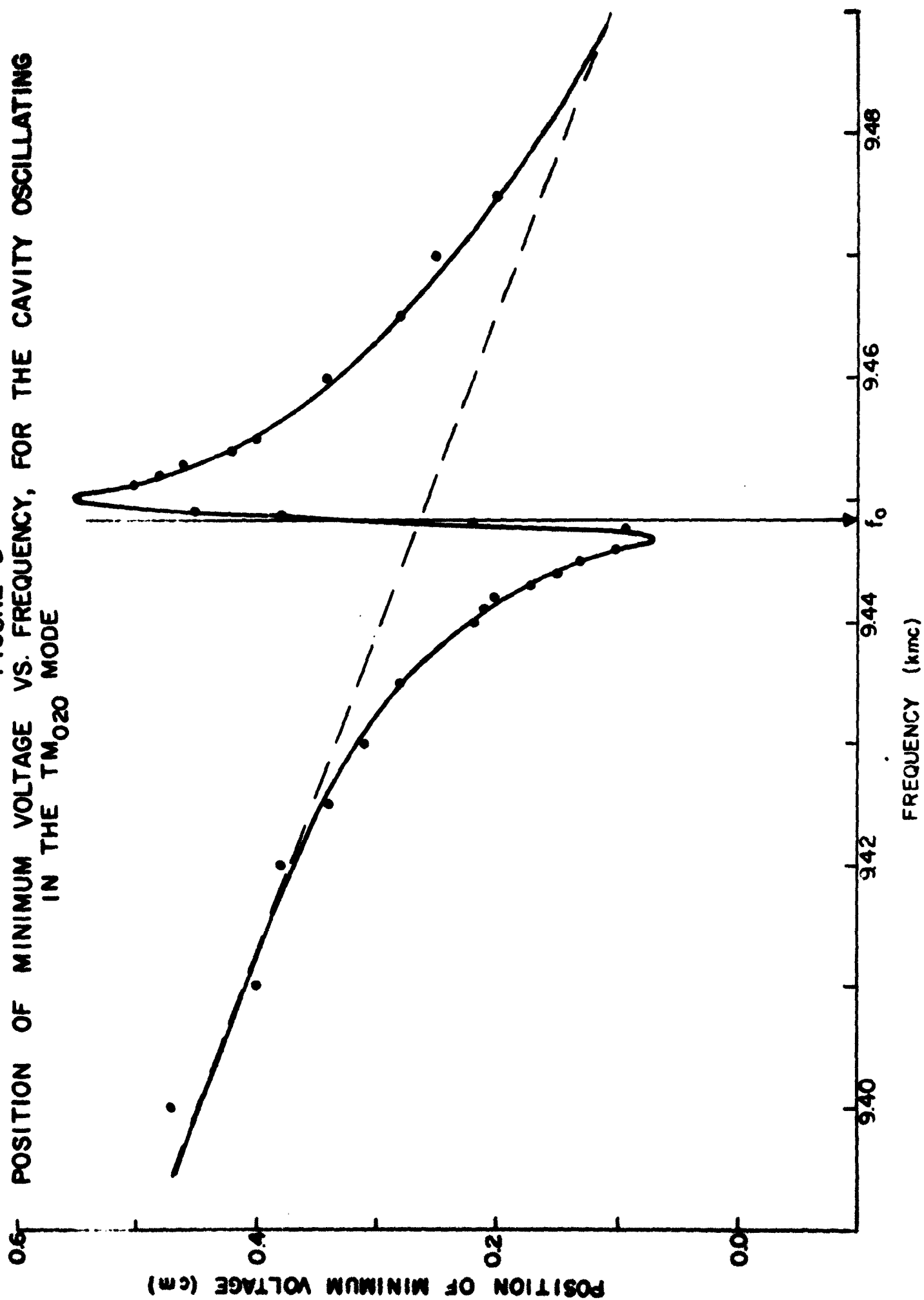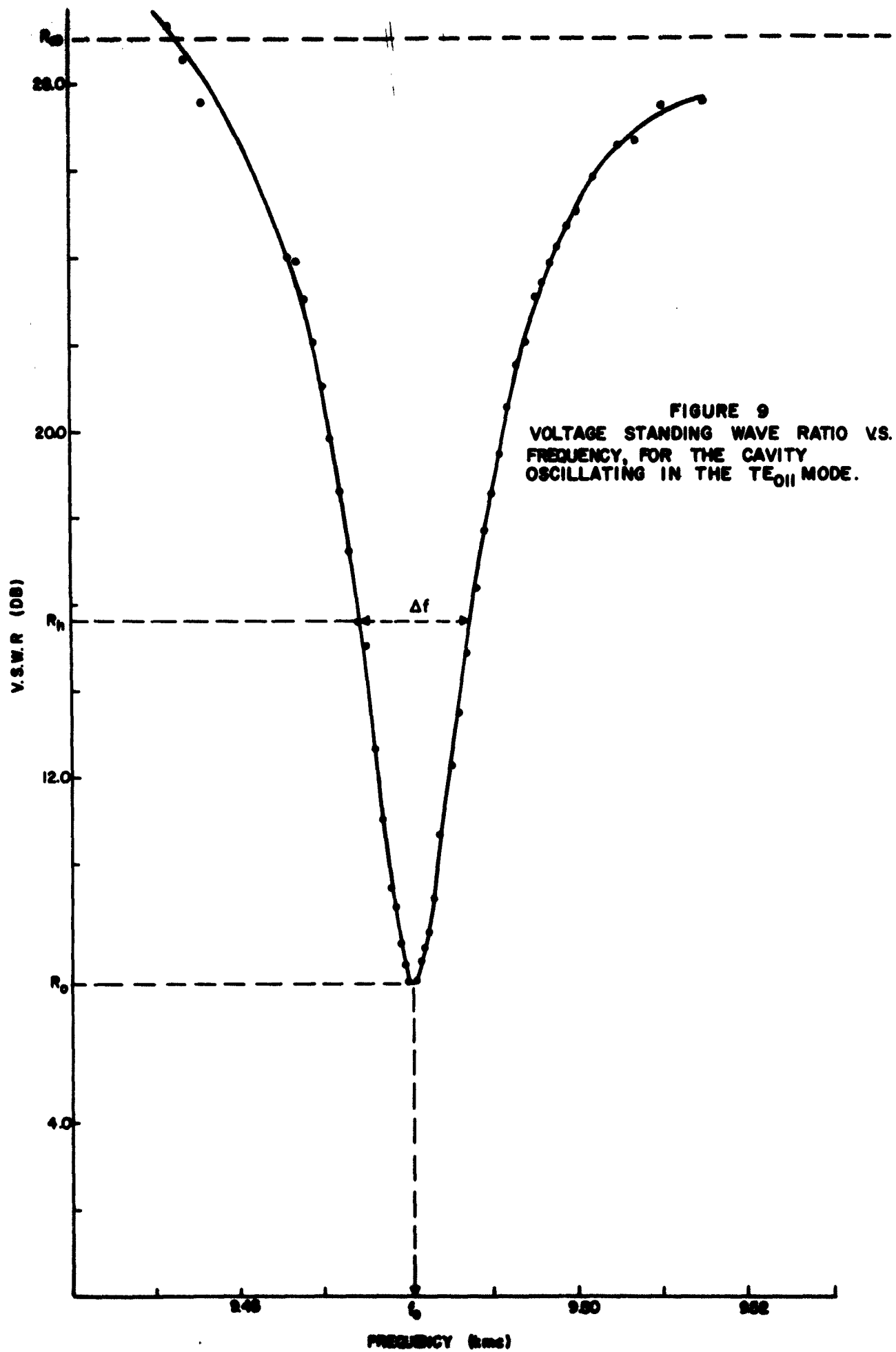
FIGURE 9
VOLTAGE STANDING WAVE RATIO V.S.
FREQUENCY, FOR THE CAVITY
OSCILLATING IN THE TE_{011} MODE.

FIGURE 10
POSITION OF MINIMUM VOLTAGE VS.
FREQUENCY, FOR THE CAVITY OSCILLATING
IN THE TE_{011} MODE.
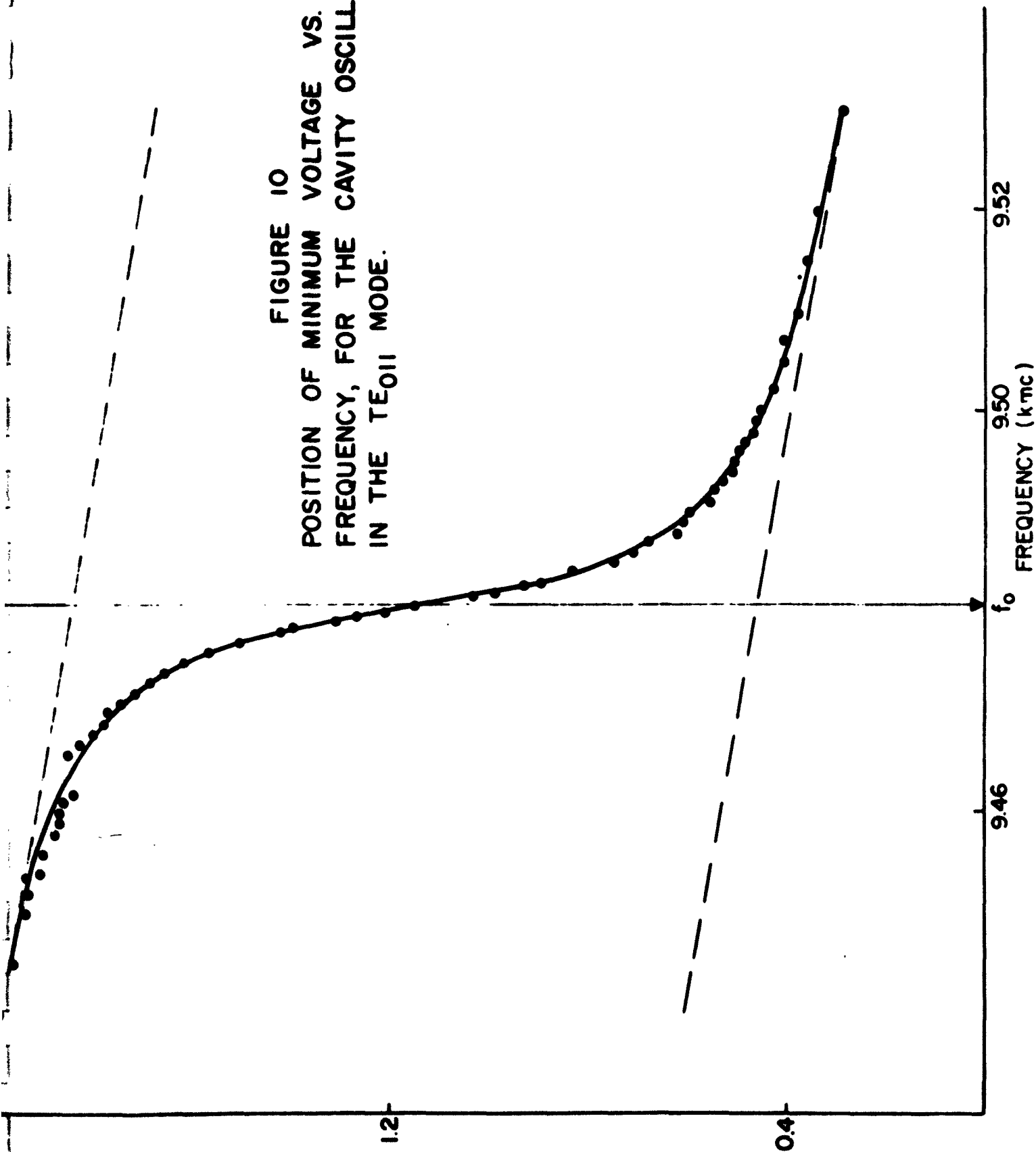
FIGURE 11

(k'/h_0) AS A FUNCTION OF THE PARAMETER m AND E_{ej}/p FOR THE TM_{020} MODE CAVITY
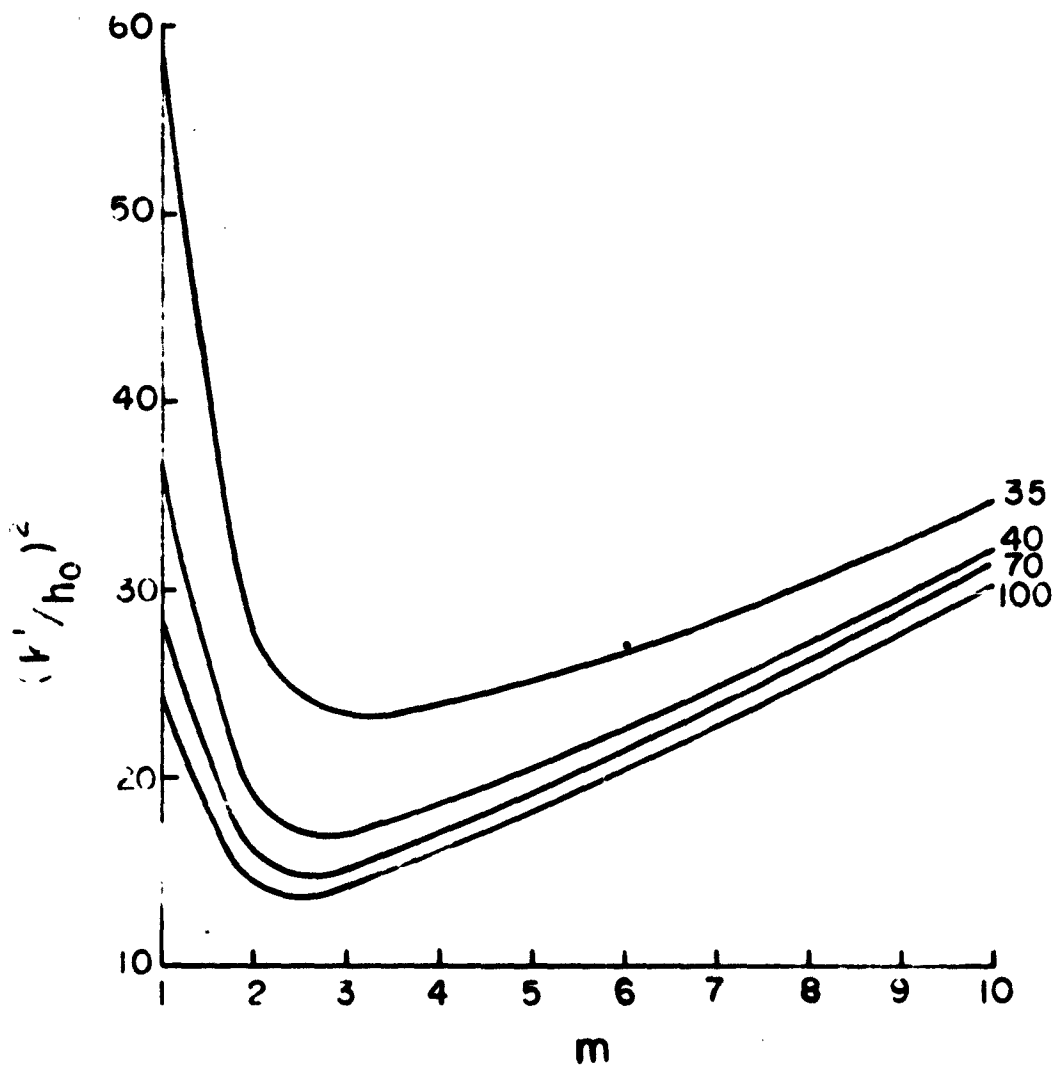
FIGURE 12

$(K'/h_0)^2$ AS A FUNCTION OF THE PARAMETER m AND E_{e0}/p FOR THE TE_{011} MODE CAVITY
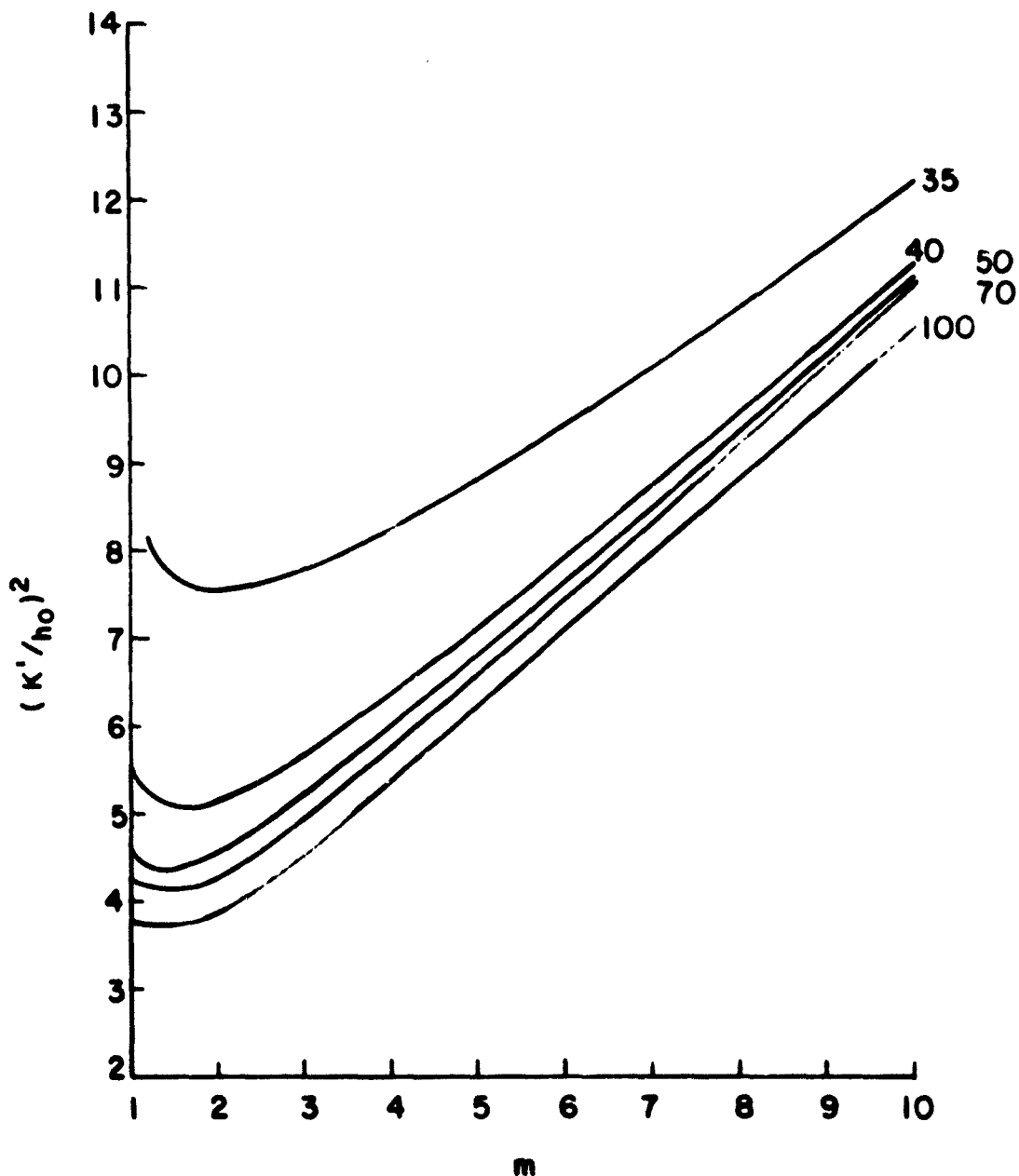
FIGURE 13

MINIMUM $(k'/h_0)^2$ VS. E_{eg}/p FOR THE TM_{020} MODE CAVITY

Vertical axis: MINIMUM $(k'/h_0)^2$

Horizontal axis: E_{eg}/p (VOLTS/cm-mm Hg)
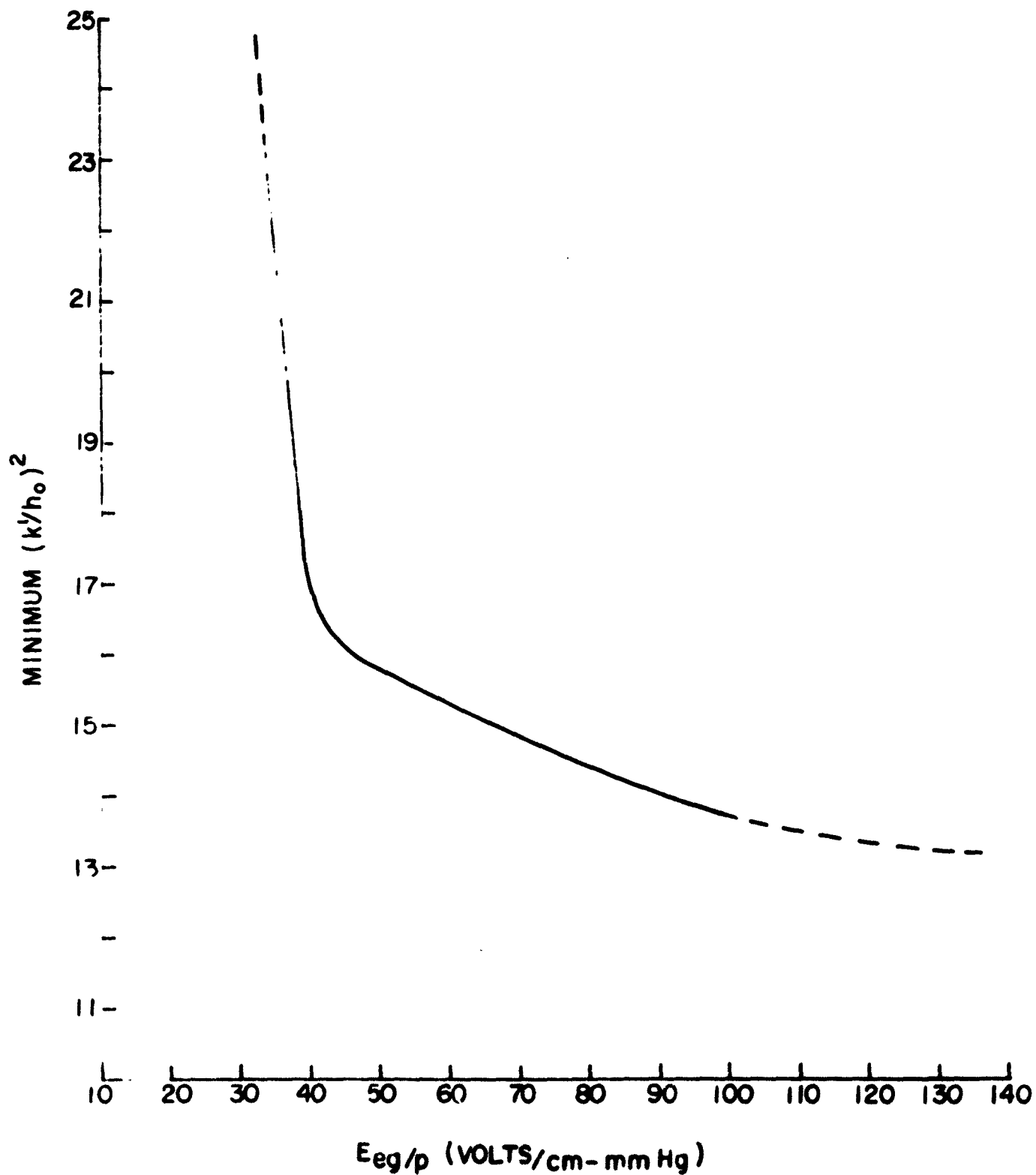
FIGURE 14
MINIMUM $(k'/h_o)^2$ VS. Eeg/p FOR THE TE_{011} MODE CAVITY

Y-axis: MINIMUM $(k'/h_o)^2$

X-axis: Eeg/p (VOLTS/cm-mmHg)
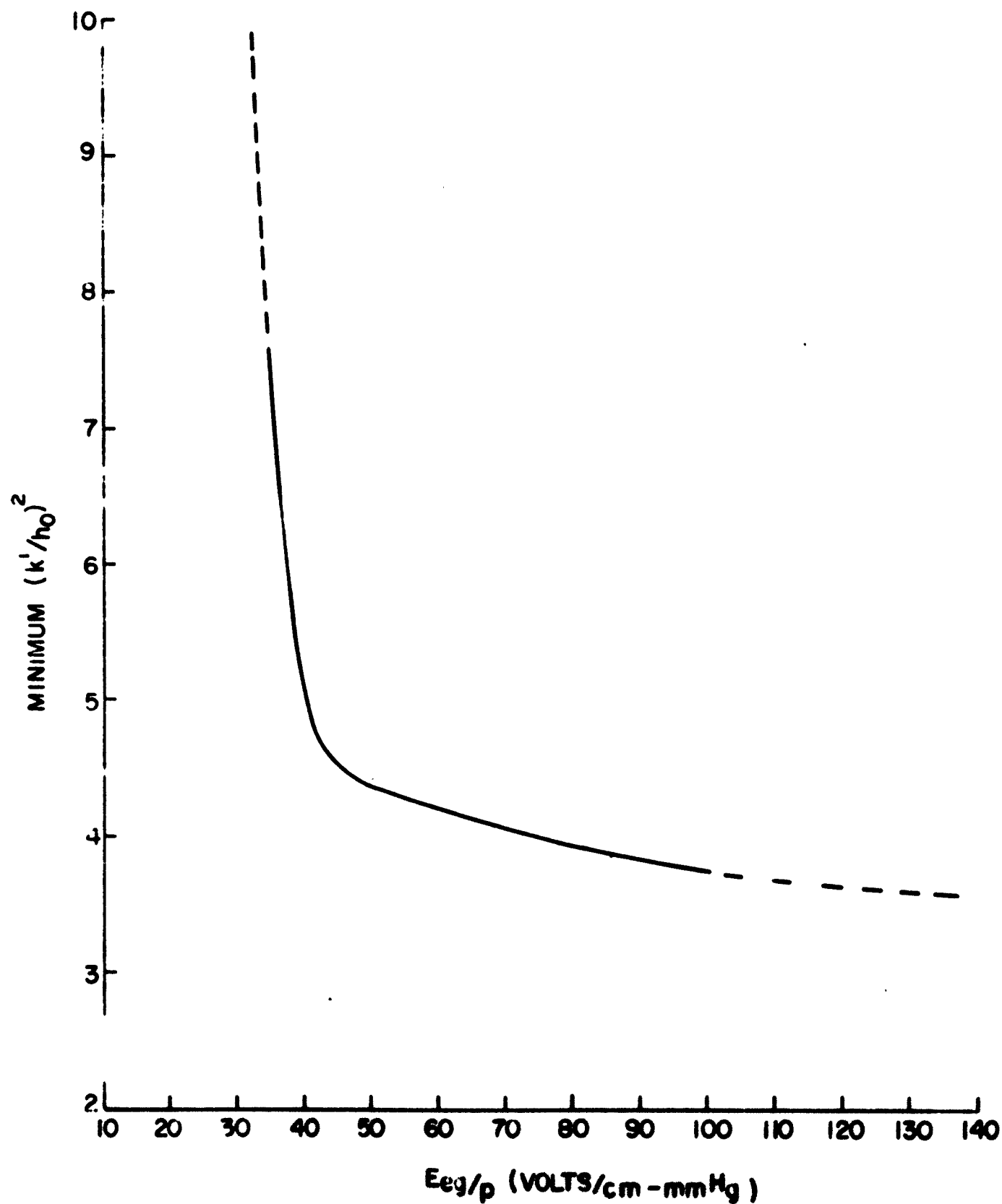
FIGURE 15

THE RATIO OF THE EQUIVALENT ELECTRIC FIELD TO THE
PRESSURE AS A FUNCTION OF THE PRODUCT OF PRESSURE
TIMES GAP DISTANCE.
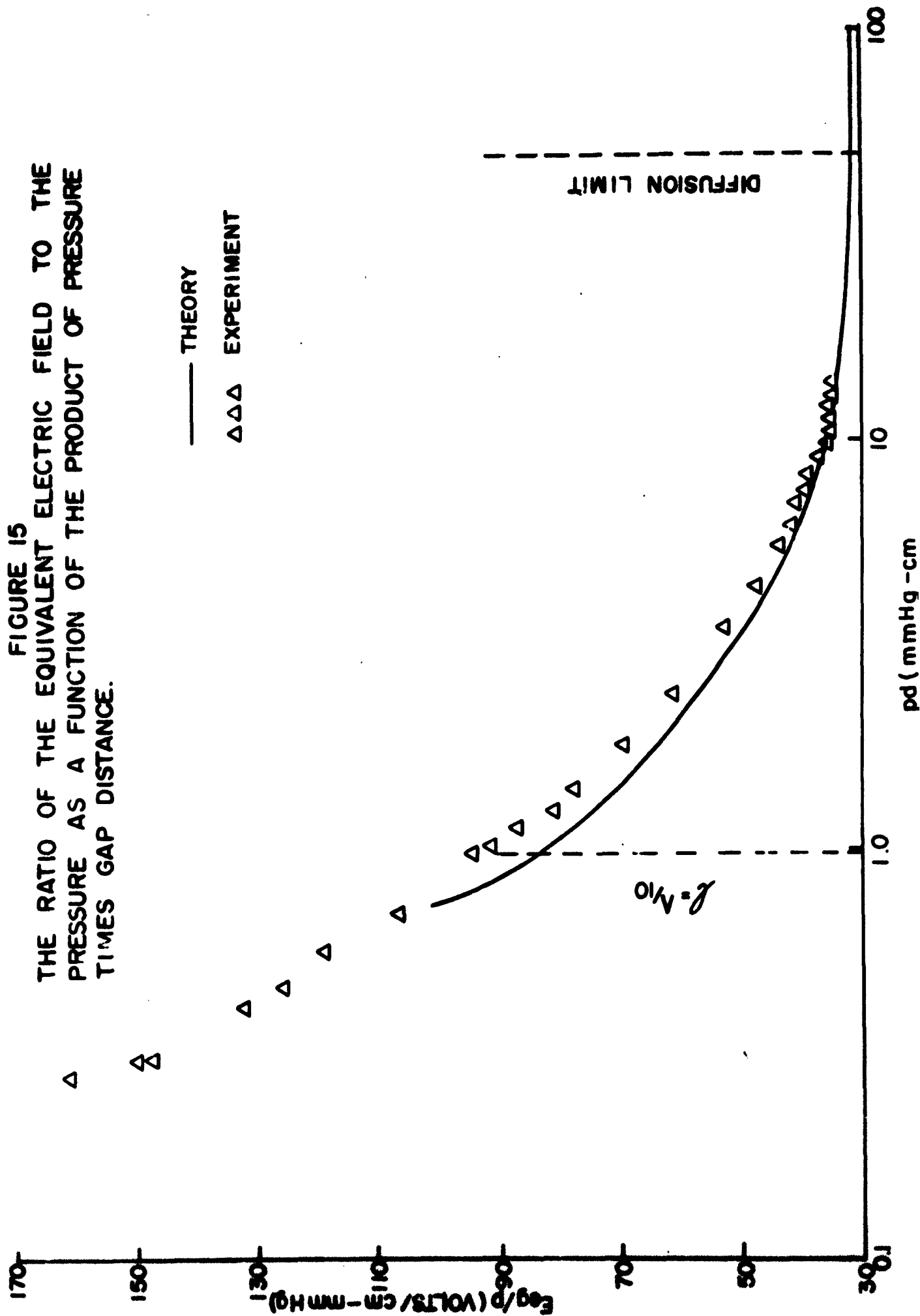
FIGURE 16

THE RATIO OF THE EQUIVALENT ELECTRIC FIELD TO THE PRESSURE AS A FUNCTION OF THE PRODUCT OF PRESSURE TIMES GAP DISTANCE.

FIGURE 17

Eeg/p VS. pAo

— UNIFORM FIELD

○ TM$_{o2o}$ MODE CAVITY

△ TE$_{o11}$ MODE CAVITY

pAo (mmHg-cm)

Eeg/p (VOLTS /cm-mmHg)

FIGURE 18

E_{eq}/p VS. $p\Lambda'$

— UNIFORM FIELD
oooo $TM_{0\infty}$ MODE CAVITY
△△△ TE_{011} MODE CAVITY

$p\Lambda'$ (mmHg-cm)

ENERGY
RELAXATION LIMIT

E_{eq}/p (VOLTS/cm-mm Hg)
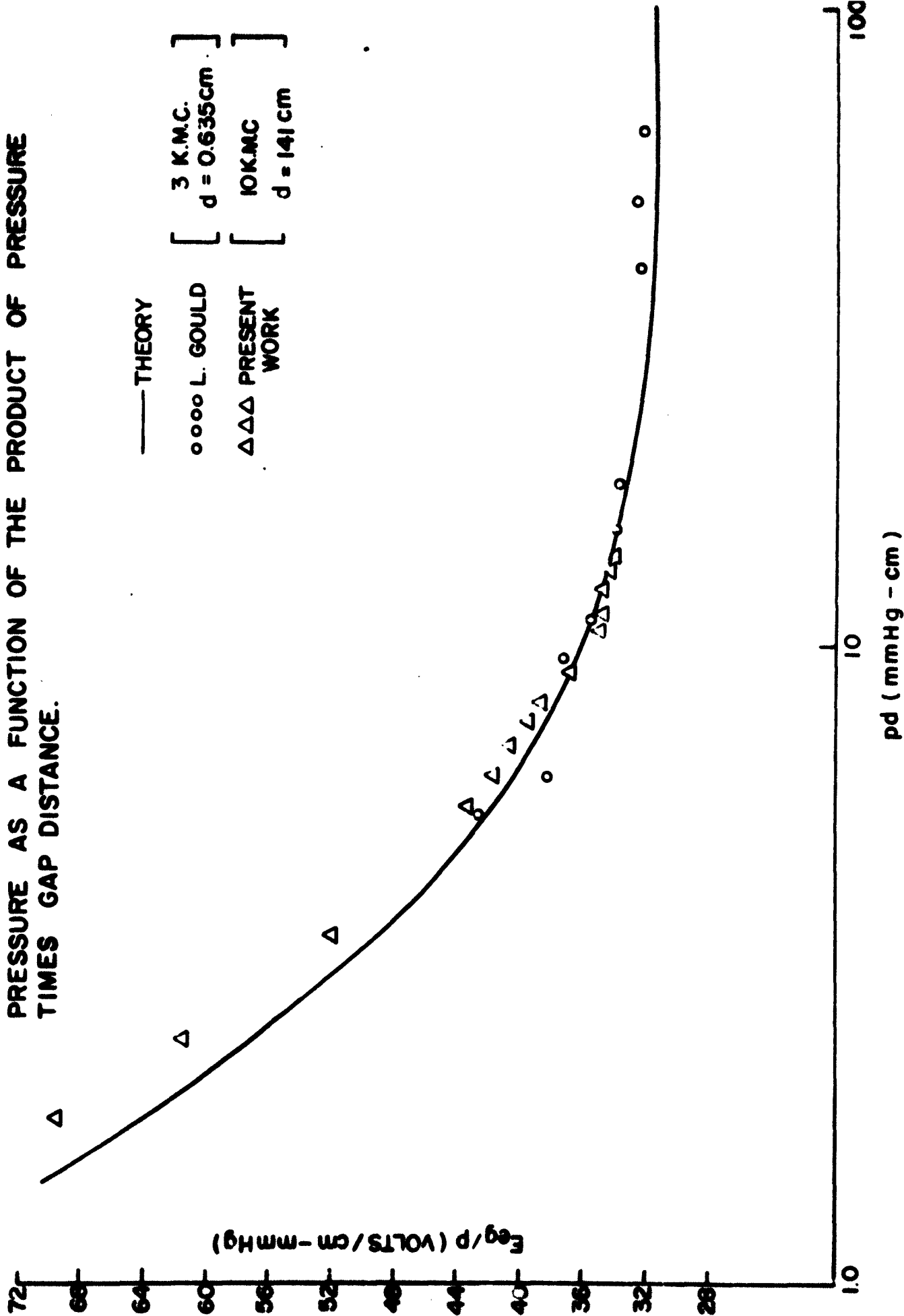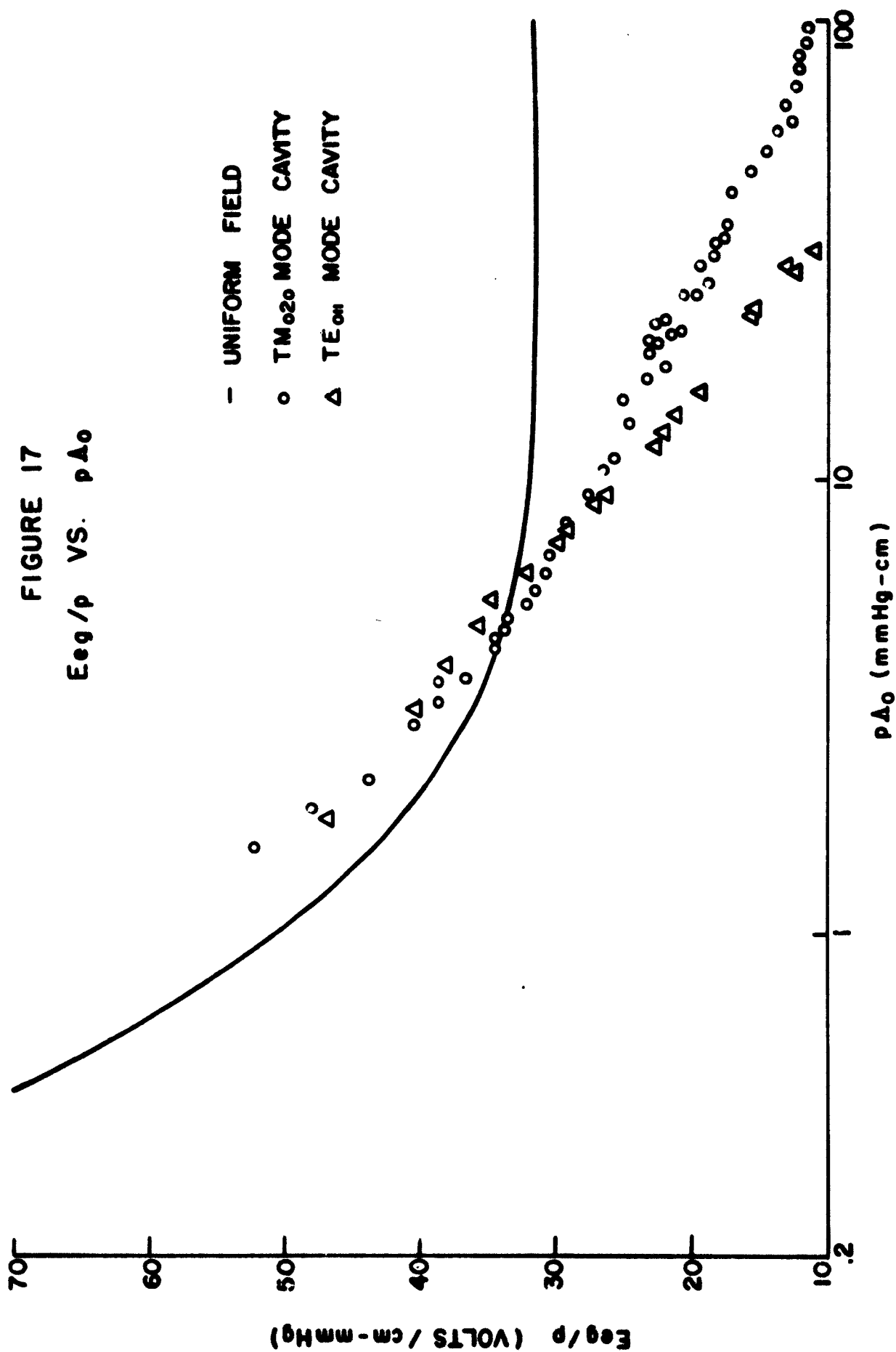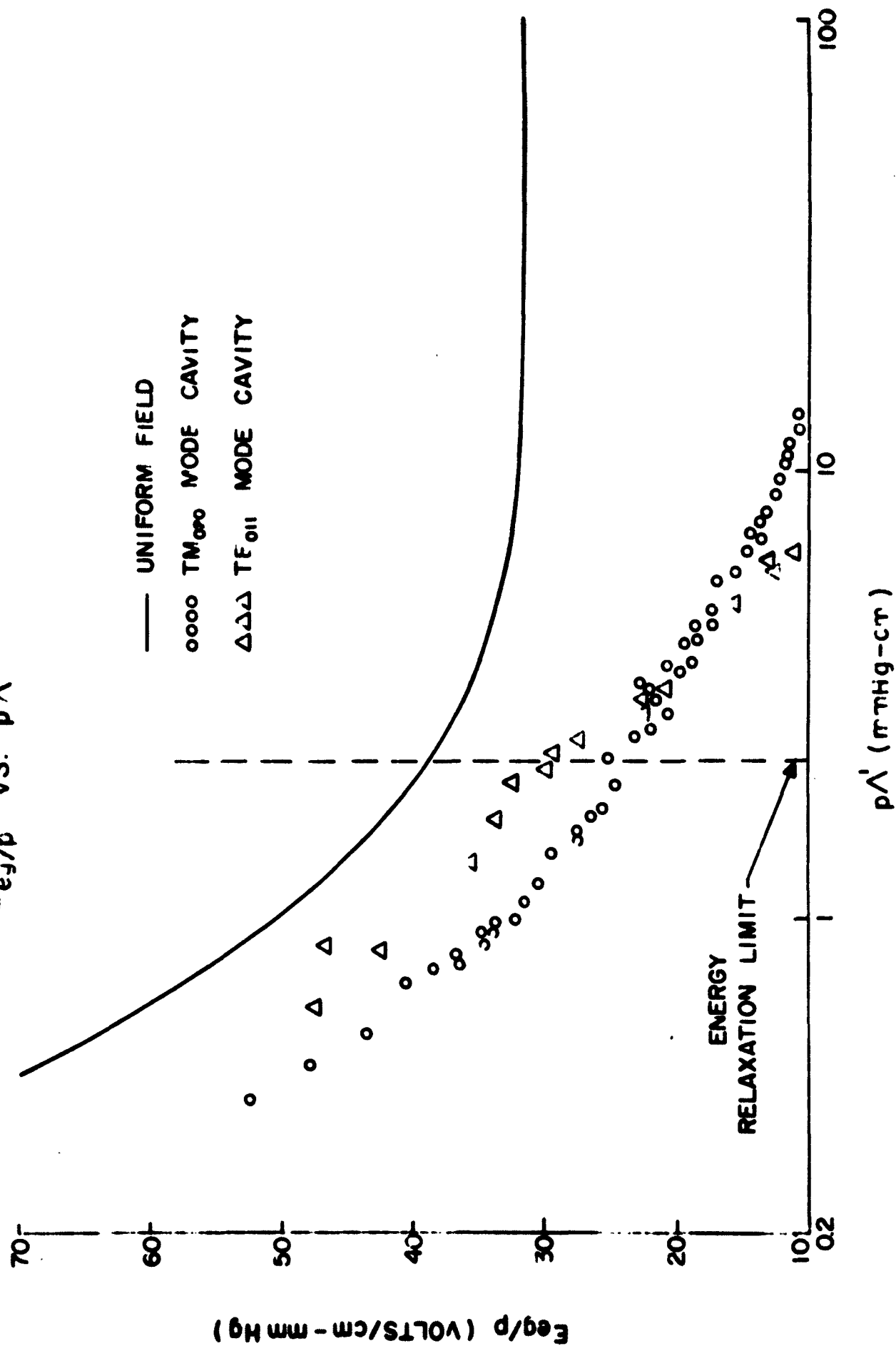
DISTRIBUTION LIST

	No. of Copies
AFMTC (AFMTC Technical Library - MU-135) Patrick Air Force Base Florida	1
AUL Maxwell Air Force Base Alabama	1
ASD(ASAPRD-Dist) Wright-Patterson Air Force Base Ohio	1
RADC (RAYLD) Griffiss Air Force Base New York ATTN: Documents Library	1
AF Missile Development Center (MDGRT) Holloman Air Force Base New Mexico	1
ARL (Technical Library) Building 450 Wright-Patterson Air Force Base Ohio	1
Commanding General USASRDL Fort Monmouth, New Jersey ATTN: Tech. Doc. Ctr. SIGRA/SL-ADT	1
Department of the Army Office of the Chief Signal Officer Washington 25, D. C. ATTN: SIGRD-4a-2	1
Commanding Officer ATTN: ORDTL-012 Diamond Ordnance Fuze Laboratories Washington 25, D. C.	1

	No. of Copies
Commanding General U.S. Army Ordnance Missile Command Redstone Arsenal, Alabama ATTN: Technical Library	1
Advisory Group on Electron Devices (AGED) Office of the Director of Defense R&E 346 Broadway, 8th Floor New York 13, New York	1
ASTIA (TIPAA) Arlington Hall Station Arlington 12, Virginia	10
National Aeronautics and Space Agency 1520 H. Street, N.W. Washington 25, D. C. ATTN: Library	1
Director Langley Research Center National Aeronautics and Space Administration Langley Field, Virginia	1
Electronic Systems Division (AFSC) Technical Information Services Div (ESAT) L. G. Hanscom Field Bedford, Massachusetts	10
Chief, Bureau of Naval Weapons Department of the Navy Washington 25, D. C. ATTN: DLI-31	2
Director (Code 2027) U. S. Naval Research Laboratory Washington 25, D. C.	2
Director, USAF Project RAND The Rand Corporation 1700 Main Street, Santa Monica, California Thru: A.F. Liaison Office	1

No. of Copies

Technical Information Office European Office, Aerospace Research Shell Building, 47 Cantersteen Brussels, Belgium	1
U.S. Army Aviation Human Research Unit U. S. Continental Army Command P. O. Box 428, Fort Rucker, Alabama ATTN: Maj. Arne H. Eliasson	1
Library Boulder Laboratories National Bureau of Standards Boulder, Colorado	2
Institute of the Aerospace Sciences, Inc. 2 East 64th Street New York 21, New York ATTN: Librarian	1
Office of Naval Research Branch Office, London Navy 100, Box 39 F.P. O. New York, N. Y.	5
Massachusetts Institute of Technology Research Laboratory of Electronis Building 26, Room 327 Cambridge 39, Massachusetts ATTN: John H. Hewitt	1
Alderman Library University of Virginia Charlottesville, Virginia	1
RADC (RALTP, A. Wiejek) Griffiss Air Force Base Rome, New York	1
RADC (RALSR, Leonard Strauss) Griffiss Air Force Base Rome, New York	1

No. of Copies

ASD (ASRMPE, Mr. Richard Rivir)   1
Wright-Patterson Air Force Base
Ohio

Bell Telephone Laboratories, Inc.   1
Whippany Laboratory
Whippany, New Jersey
ATTN: Technical Information Library

Technical Library   1
G.E. TWT Product Section
601 California Avenue
Palo Alto, California
ATTN: Verna Van Velzer, Librarian

General Electric Advanced Electronics Center   1
Tompkins County Airport
Ithaca, New York
ATTN: Mr. F. M. Perry

Sylvania Electric Products, Inc.   1
Electronic Defense Laboratory
123 N. Whisman Road
Mountain View, California
ATTN: Library

Division of Sperry Rand Corporation   1
Sperry Gyroscope Company
Great Neck, Long Island, New York
ATTN: Florence W. Turnbull
       Engineering Librarian

General Electric Company, Power Tube Department   1
Electronic Components Division
Building 269, Room 205, One River Road
Schenectady 5, New York

Directorate of Development Planning   1
DCS Research & Technology
AFRDP-S (Michael Lorenzo)
Hq. USAF
Washington 25, D. C.

No. of Copies

General Telephone & Electronics Laboratories, Inc.   1
Bayside Laboratories
Bayside 60, New York
ATTN: D. Lazare, Mgr., Proj. Adm.

Eitel-McCullough, Inc.   1
798 San Mateo Avenue
San Bruno, California
ATTN: Donald H. Preist

Varian Associates   2
611 Hansen Way
Palo Alto, California
ATTN: Dr. Richard B. Nelson

Varian Associates   1
611 Hansen Way
Palo Alto, California
ATTN: E. W. Herold, Vice President, Research

Lockheed Aircraft Corporation   1
Missiles & Space Division
Technical Information Center
3251 Hanover Street
Palo Alto, California
ATTN: W. A. Kozumplik, Manager

AVCO Manufacturing Company   1
2385 Revere Beach Parkway
Everett 49, Massachusetts
ATTN: Dr. A. R. Kantrowitz

Philips Laboratories   1
Division of North American Philips Co., Inc.
Irvington on Hudson, New York
ATTN: William P. Arnett, Security Officer

Research Technology Associates, Inc.   1
100 Ladge Drive
Electronic Park at Avon
Avon, Massachusetts
ATTN: J. Babakian

No. of Copies

	No. of Copies
Raytheon Company Norwood Plant 415 Providence Highway Norwood, Massachusetts ATTN: L. C. Edwards	1
ARO, Inc. AEDC Library Arnold Air Force Station, Tenn.	2
Rocketdyne 6633 Canoga Avenue Canoga Park, California ATTN: Dr. R. H. Boden-Department 584-370	1
Aero Chem. Research Laboratories, Inc. P. O. Box 12 Princeton, New Jersey ATTN: Dr. Calcote	1
Litton Systems, Inc. 336 N. Foothill Road Beverly Hills, California ATTN: Space Sciences Laboratory	1
Hughes Research Laboratories Malibu, California ATTN: Dr. M. R. Currie	1
Westinghouse Electric Corp. Box 284 Elmira, New York ATTN: D. C. Buck, Head Microwave Research & Development Section	1
American Systems Incorporated 1625 East 126th Street Hawthorne, California ATTN: M. D. Adcock, Director Electromagnetic Systems Division	1
Linde Company 1500 Polco Street Speedway 24, Indiana ATTN: Dr. M. Stern	1

	No. of Copies
General Telephone & Electronics Laboratories, Inc. Microwave Physics Laboratory 1015 Corporation Way Palo Alto, California ATTN: Librarian	1
S-F-D Laboratories, Inc. 800 Rahway Avenue Union, New Jersey	1
F. J. Liberatore, Code 7420 U. S. Naval Research Lab. Washington 25, D. C.	1
New York University Institute of Mathematical Sciences 25 Waverly Place, Room 802 New York 3, New York ATTN: Dr. Morris Kline	1
Stanford University Stanford Electronics Laboratories Stanford, California ATTN: Dr. Dean A. Watkins	1
Stanford University Microwave Laboratory W. W. Hansen Laboratories of Physics Stanford, California ATTN: Dr. Marvin Chodorow	1
California Institute of Technology 1201 E. California Pasadena, California ATTN: Dr. S. S. Penner	1
Polytechnic Institute of Brooklyn Microwave Research Institute 55 Johnson Street Brooklyn, New York ATTN: Dr. N. Marcuvitz	1
The Ohio State University Department of Physics 174 W. 18th Avenue Columbus 10, Ohio ATTN: Prof. M. L. Pool	1

Contract No. AF19(604)-7388
Final Report

University of Maryland   1
College Park
Maryland
ATTN: Dr. J. M. Burgers

Cornell University   1
Ithaca, New York
ATTN: W. R. Sears

Electrical Engineering Research Laboratory   1
University of Illinois
Urbana, Illinois
ATTN: Dr. A. A. Dougal

Stevens Institute of Technology   1
Hoboken, New Jersey
ATTN: Dr. Bostick

University of Mississippi   1
University, Mississippi
ATTN: Mr. Thomas Tullos

Remaining copies to:
Electronic Systems Division (AFSC)
Technical Information Services Div (ESAT)   7
L. G. Hanscom Field
Bedford, Massachusetts